

Structural evolution of the sodium cluster anions Na_{20}^- - Na_{57}^-

Bernd Huber and Michael Moseler*

*Freiburg Materials Research Center, Stefan-Meier-Straße 21, 79104 Freiburg, Germany
and Fraunhofer Institut für Werkstoffmechanik, Wöhlerstraße 11, 79108 Freiburg, Germany*

Oleg Kostko and Bernd v.Issendorff†

*Fakultät für Physik, Universität Freiburg, Hermann-Herder-Straße 3, 79104 Freiburg, Germany
(Received 16 September 2009; published 17 December 2009)*

Sodium clusters anions Na_n^- ($n=20-57$) have been studied by low-temperature photoelectron spectroscopy (PES) and density-functional theory calculations. The geometrical structures of the clusters were determined by a genetic algorithm search and the optimization of a large number of candidate structures. For most of the sizes the calculated density of states of the lowest-energy structures and the measured photoelectron spectra are in excellent agreement, indicating that the correct ground-state structures were found. In the studied size range the sodium clusters follow a simple growth pattern. From Na_{20}^- to Na_{34}^- a 19 atom double-icosahedral core is stepwise decorated by a 15 atom equatorial belt. The resulting D_{5h} Na_{34}^- is then capped by an anti-Mackay overlayer in the size range Na_{34}^- to Na_{44}^- . From Na_{52}^- to Na_{55}^- a Mackay overlayer on a 13 atom icosahedron core is completed. Na_{56}^- and Na_{57}^- result from the 55 atom icosahedron by incorporation of additional adatoms into the outer Mackay layer. Comparison of the *ab initio* derived structures with results from jellium or Nilsson models reveal that for sizes below Na_{40}^- the overall cluster shapes are rather accurately predicted by these simple free-electron models. For larger sizes the agreement is less good, as here optimum atomic packing plays a stronger role. This is most obvious close to size 55, where the icosahedral shell closing leads to a spherical shape of the cluster, whereas the free-electron models predict significant distortions.

DOI: [10.1103/PhysRevB.80.235425](https://doi.org/10.1103/PhysRevB.80.235425)

PACS number(s): 36.40.Mr, 33.60.+q, 73.22.-f

I. INTRODUCTION

Clusters and nanoparticles can have very different characteristics than the corresponding bulk material, which makes them very attractive objects both for applications as for fundamental research. An indispensable prerequisite for an understanding of their properties is the knowledge of their exact geometrical structure. An enormous effort therefore has been put into structural determinations of clusters in the recent years.^{1,2} For many materials cluster structures are known by now, although in most cases still only for small particles with up to roughly 20 atoms or for very large ones with several hundred atoms.^{2,3} In two recent papers we have presented a combined experimental and theoretical study of the structure of sodium cluster anions Na_n^- in the size range $n=4-19$ atoms⁴ and $n=39-350$ atoms.⁵ Here we present results for the intermediate range $n=20-58$, thereby closing the gap between the two size ranges and making sodium clusters the first system for which structural information is available from the few atom up to the several nanometer diameter size regime.

As bulk sodium is the best representative of a free-electron metal,⁶ sodium clusters can be expected to be rather simple quantum systems. Indeed free-electron models, which completely neglect the atomic structure of the clusters, have been very successful in describing the size dependence of, e.g., binding energies, ionization potentials, and absorption cross sections of sodium clusters.^{7,8} This is especially true for hot liquid clusters, that, is for clusters with room temperature or higher.⁹ Recently we demonstrated that in the size range $n=4-19$ even in their ground state the overall shape of the clusters is completely determined by the form of

the extended electronic wave functions.⁴ For larger sizes with $n=55-350$ we have shown that the ground-state structures in most cases are strongly influenced by packing patterns of the atoms which optimize the average coordination number.⁵ Here we conclude this discussion by looking at the structure of clusters in the transition size range.

The paper is organized as follows. It starts with a brief description of the theoretical and experimental methods. Then the measured photoelectron spectra are presented and compared to the calculated density of states (DOS) of the lowest-energy structures found, thereby verifying (or falsifying) the structure determination. Finally the overall shape of the clusters as evaluated from the cluster structures is discussed in the light of the predictions of simple free-electron models.

II. METHODS

A. Theory

In order to find the structural ground states of the sodium cluster anions, density-functional theory (DFT) in the framework of the local spin-density approximation (LSD) for the description of the electronic ground-state Born-Oppenheimer (BO) surface was employed. The Kohn-Sham equations were solved for the sodium $3s$ valence electrons using the BO-LSD-molecular-dynamics method.¹⁰ Within this method the Kohn-Sham orbitals were expanded in a plane-wave basis with a 10 Ry cutoff. The electron-ion interaction was described by a nonlocal pseudopotential¹¹ with p as the local (core radius $2.6a_0$) and s as the nonlocal component (core radius $2.45a_0$). Exchange and correlation were treated within

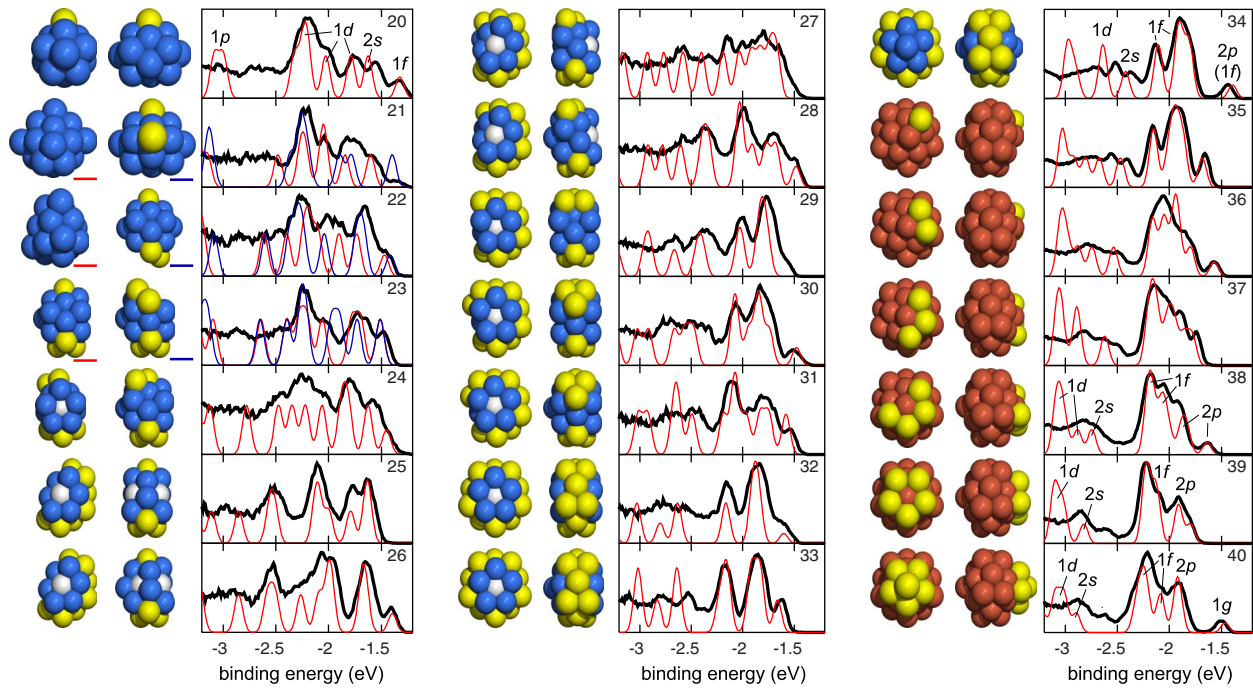


FIG. 1. (Color online) Ground-state structures of Na_{20-40}^- and the comparison of the corresponding calculated DOS (red or shaded line) and the measured photoelectron spectra (thick black line). Two perpendicular views of the clusters are provided except for Na_{21-23}^- where two quasidegenerate isomers are depicted. For these three sizes, the DOS of the second lowest isomer is plotted with a blue (or dark) line. Atoms added to the double icosahedron basic unit (outer atoms: dark or blue, central atom: white) are colored in yellow (or light gray). For Na_{35-40}^- , atoms of the Na_{34}^- -core are colored in red (or shaded). The structures of the lowest isomers for Na_{21-22}^- do not follow the simple icosahedral growth pattern.

LSD enhanced by an additional generalized gradient correction (GGA).¹²

The BO surfaces of the clusters were scanned for the global minimum employing a modified single-parent genetic algorithm.¹³ Each candidate structure was relaxed until forces were smaller than $0.005 \text{ eV}/\text{\AA}$. The calculated total energy was then used as the fitness parameter in the genetic algorithm iterations. Additionally ground-state structures of different empirical potentials¹⁴ and modifications of them were used as starting points for the relaxation.

For the structures with the lowest-energy photoelectron spectra were then simulated by shifting the calculated DOS so that the highest molecular-orbital (HOMO) eigenvalue coincides with the calculated vertical detachment energy. The calculated spectra were convoluted with Gaussians of width $\sigma=0.04 \text{ eV}$ in order to facilitate the comparison with the measured spectra. Details of this procedure and its validity have been discussed earlier.⁴ For the determination of jellium type quantum numbers the overlap of the Kohn-Sham orbitals with cluster centered spherical harmonics has been calculated.

B. Experiment

The experimental apparatus used in this study is the same as in recent investigations.^{4,5,15,16} The sodium clusters are produced in a gas aggregation source, where they are negatively charged by a pulsed discharge near the exit of the aggregation tube. After leaving the source the clusters are

trapped in a liquid nitrogen cooled rf octupole trap, where they are thermalized by collisions with background helium. Photofragmentation experiments on cationic clusters thermalized in this way showed by comparison to existing results of caloric measurements¹⁷ that the temperature of the clusters typically is $100 \pm 5 \text{ K}$, which is assumed to be the temperature of the cluster anions as well. After leaving the octupole the thermalized clusters are extracted into a double reflectron time-of-flight mass spectrometer, where they are size selected, decelerated and finally irradiated by a laser pulse in the interaction region of a magnetic bottle type time-of-flight photoelectron spectrometer. The spectrometer has an energy resolution of about $E/dE=40$ and has been calibrated by measuring the known spectrum of the Pt^- anion. For the photodetachment a XeCl-excimer laser ($h\nu=4.02 \text{ eV}$) is used. The electron time-of-flight spectra have been accumulated in a digital oscilloscope (in most cases for about 20 000 laser shots), and finally converted into binding-energy spectra.

III. RESULTS AND DISCUSSION

The measured photoelectron spectra are shown in Figs. 1 and 2. Like the spectra of the smaller or larger clusters published earlier,^{4,5} they are strongly structured, indicating a highly discretized DOS. Again the electron shell structure is directly visible for some sizes; the shell closures at electron numbers 20, 34, 40, and 58 lead to the appearance of a new shell at the next higher size, that is, at Na_{20}^- , Na_{34}^- , Na_{40}^- , and

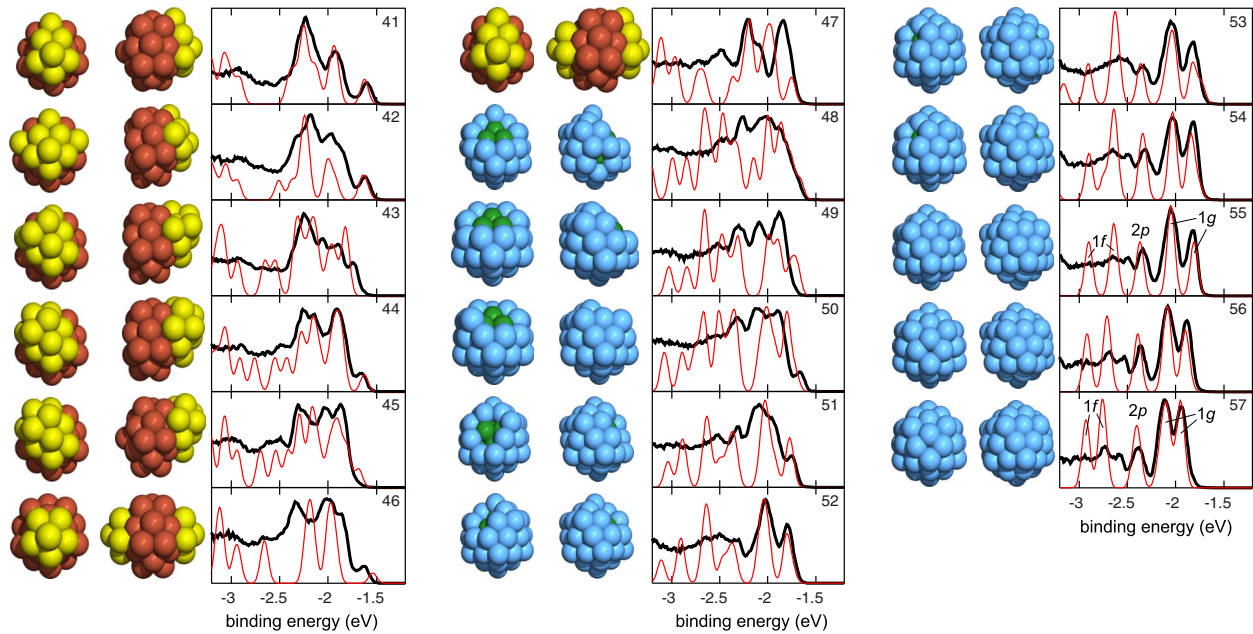


FIG. 2. (Color online) Ground-state structures of Na_{41}^- – Na_{57}^- and the comparison of related DOS (red or shaded line) and photoelectron spectra (black thick line). For Na_{48}^- – Na_{57}^- , atoms of the icosahedral Na_{13} core are colored in dark green (or dark gray); atoms of the outer shell are shown in light blue (or light gray).

Na_{58}^- (not shown here). For these and neighboring sizes spherical jellium quantum numbers have been assigned to the peaks visible in the calculated DOS (in the case of Na_{34}^- two assignments are given for the uppermost state, which has a mixed p/f character). In the photoelectron spectra this electron shell structure can be clearly seen only close to the threshold, as for higher binding energies (here more than about 1 eV below threshold) only very broad and weak peaks are observed, which are superimposed onto a strong unstructured background. For these lower lying states the photodetachment cross section obviously is small; furthermore the very short lifetime of the hole produced upon photoemission causes a strong broadening of the peaks. Finally inelastic scattering of the photoelectrons in the cluster and Auger-like emission processes lead to a dominant intensity of low kinetic-energy photoelectrons which do now reflect the DOS. Therefore the most significant part of a photoelectron spectra is always the part close to the threshold.

The geometries of the lowest-energy structures found for each size are indicated in Figs. 1 and 2. The corresponding coordinate files are available in Ref. 21. The electronic densities of states of the structures are shown as red and blue (or light and dark gray) lines in the plots of the photoelectron spectra. Note that the comparison between theoretical and experimental spectra is meaningful only in the uppermost (low binding-energy) part. This is due to the effects mentioned above and to the fact that the simulated spectra overestimate binding energies of lower lying states, which leads to a systematic mismatch of measured and calculated spectra at higher binding energies.²² As the DOS is very sensitive to the nuclear structure of the cluster, a good agreement between the DOS of the lowest-energy isomer found and the experimental spectrum gives strong evidence that the correct structure has been found. This is of course not a proof in a

mathematical sense; one can never exclude the existence of an even lower energy isomer with a very similar DOS. In the next section we will now discuss the geometries found and their experimental corroboration in detail.

A. Geometrical structure evolution

For almost all of the clusters shown in Fig. 1 the basic building block is a 19-atom double icosahedron, with the remaining atoms forming an equatorial belt around the waist of this core. The core double icosahedron does not necessarily stay intact in this buildup sequence; in many cases one or two of its tip atoms (the end atoms of its central linear tetramer) are transferred to the equatorial ring, which optimizes the average atom coordination number and changes the overall cluster sphericity. For the same reason in some cases an atom out of one or two of the outer five-membered rings of the core is transferred to the waist position.

This growth pattern starts at size 20. While for the electronically closed-shell Na_{19}^- the prolate double icosahedron structure is energetically unfavored,⁴ the lowest-energy structure found for Na_{20}^- is exactly this double icosahedron with one capping atom attached to its side. The excellent agreement of theoretical DOS and measured photoelectron spectra (Fig. 1) indicates that this structure indeed represents the ground-state structure.

For Na_{21}^- our calculations revealed two quasidegenerate ground-state structures with an energy difference of only $\Delta E = 20$ meV (left and right structure in Fig. 1). One of these is the double icosahedron with two capping atoms, while the other one is a C_{2v} -structure based on a heavily distorted 13 atom decahedron. The experimental spectrum can be well reproduced by a weighted superposition of the DOS of both isomers. The situation is similar for Na_{22}^- and Na_{23}^- , for each

of which again two quasidegenerate ground states were found (with an energy difference ≤ 20 meV). One isomer of Na_{22}^- is a triply capped double icosahedron, while the other one is irregular. For Na_{23}^- both isomers are capped double icosahedra; in the lower energy structure the four additional atoms and one of the tip atoms of the 19 atom core are placed onto the waist, while for the second isomer two core atoms (the tip atom and an adjoining atom from a five-membered ring) are transferred to the waist. Note that the resulting electronic densities of states exhibit significant differences, although the two structures differ only by the displacement of two atoms. As the DOS of the second isomer exhibits a peak at 1.9 eV, where the experimental spectrum shows a minimum, one can directly conclude that in spite of the calculated quasidegeneracy the relative abundance of the second isomer must be small.

For most of the following cluster sizes up to Na_{40}^- the good to very good agreement between the experimental and theoretical spectra provides strong evidence for the correct determination of the ground-state structures. The growth scheme is very simple: the structure of a cluster Na_n^- in most cases is just the one of the previous cluster Na_{n-1}^- with one atom added. Only occasionally a rearrangement of a few other atoms occurs. A geometric shell closing is reached at size 34, which has D_{5h} symmetry and consists of the 19 atom double icosahedron decorated by three five-membered rings. The structures from Na_{34}^- to Na_{40}^- are constructed by consecutive capping of this Na_{34}^- with a six-atom pentagonal pyramid, resulting in a rather spherical structure for the electronically closed-shell Na_{39}^- and a slightly prolate shape for Na_{40}^- . Note that Na_{38}^- does not adopt the structure of a truncated octahedron, which is the ground state of several empirical potentials.¹⁴ This geometry would lead to a much simpler DOS than the one observed,^{16,23} and lies 0.5 eV higher in energy than the Na_{38}^- structure found here.

Figure 2 depicts the geometric and electronic structure in the size range Na_{41}^- - Na_{57}^- . The ground-state structures of Na_{41}^- and Na_{42}^- continue the Na_{20}^- - Na_{40}^- growth pattern by capping the perimeter of the pentagonal pyramid subunit of the Na_{40}^- cluster. For $n=42-44$ a tip atom of the 19 atom core (opposite the pentagonal pyramid) is transferred toward the pyramid perimeter. The densities of states of both the Na_{41}^- and the Na_{42}^- ground state agree well with the measured photoelectron spectra. For Na_{43}^- the agreement is not as good, which indicates that the true ground state probably has a slightly different structure.

Capping the faces of the pentagon pyramid results in the lowest-energy structure for Na_{44}^- , the DOS of which is again in very good agreement with the PES results. All other isomers found are at least 100 meV higher in energy. Adding again the tip atom of the 19 atom core leads to the lowest-energy structure of Na_{45}^- we were able to find. The poor agreement of DOS and PES results for this size and also for the following sizes $n=46-51$ suggests, however, that these structures are not the true ground states. It seems that in this size range a completely different building scheme prevails, but despite extensive computational sampling we did not succeed in finding it. For the sizes $n=52-55$ the structural identification was straightforward again. It is well established that Na_{55}^- is a closed-shell Mackay icosahedron.⁵ By

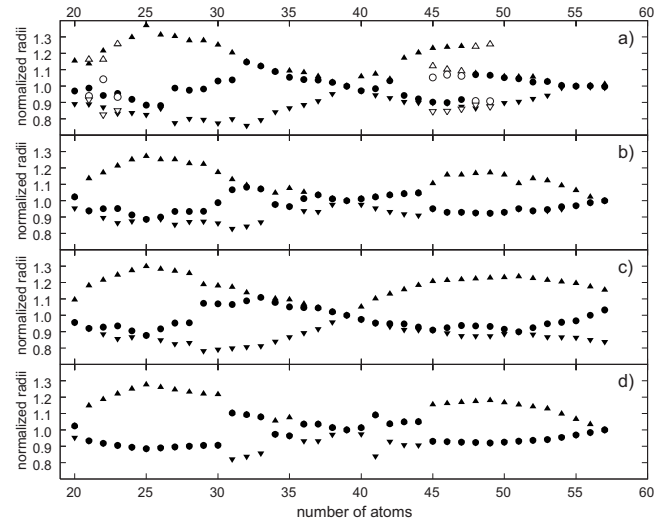


FIG. 3. Normalized radii ($R_x, R_y, R_z=1$) along the principal axes for Na_{20-57} . (a) Radii of the ground-state structures (filled symbols) from the DFT calculations. For Na_{21-23}^- radii of the second lowest isomer and for Na_{45-49}^- radii of the lowest Mackay or anti-Mackay structure are shown (open symbols). (b) Optimal radii for the triaxial jellium model (Ref. 18). (c) Optimal radii for the ellipsoidal shell model (Ref. 19). (d) Optimal radii for the Clemenger-Nilsson model (Ref. 20). Triangles represent the largest and the smallest radius, circles represent the intermediate radius.

removing atoms from this structure (a vertex atom for 54, two opposing vertex atoms for 53, a vertex atom and an opposing vertex-edge dimer for 52) we obtain lowest-energy geometries for which again an excellent agreement of DOS and PES results is obtained. We finish the structure discussion with the two sizes Na_{56}^- and Na_{57}^- , which are close to and at the electronic shell closure occurring for 58 valence electrons. As has been discussed already in Ref. 5, due to the tendency of electronically closed-shell clusters to have a spherical shape the extra atoms are pushed into the surface of the icosahedron. This results in three almost equal radii of inertia and an energy gain of 0.1 eV with respect to structures where the additional atoms occupy places on the surface.

B. Cluster deformation

Obviously the geometrical cluster structures in this size range follow something not unlike a hard-sphere packing scheme. It is an interesting question whether their overall shape nevertheless is still in accordance with simple free-electron model prediction.

In order to characterize the cluster shapes we have calculated the radii of inertia from an analysis of the principal moments of inertia for the atomic coordinates. The radii of the DFT ground-state geometries found are presented in Fig. 3(a) and compared to radii from the triaxial jellium model¹⁸ [Fig. 3(b)], from the ellipsoidal shell model¹⁹ [Fig. 3(c)] and from the Clemenger-Nilsson model (CNM) (Ref. 20) [Fig. 3(d)]. Note that the ellipsoidal shell model differs from the CNM by the extension to triaxial deformations but neglects the angular-momentum-dependent perturbation of the CNM.

Starting from the spherical Na_{19}^- (not shown here, see Ref. 4) the *ab initio* derived clusters get prolate, in agreement with all three simple models. The maximum deformation is reached at Na_{25}^- , again in accordance with all models. For Na_{27}^- , the *ab initio* cluster shape turns to triaxial, consistent with the jellium and the ellipsoidal model (CNM can only describe biaxial shapes). From Na_{32}^- to Na_{34}^- the *ab initio* clusters prefer an oblate shape, and then slowly converge toward a spherical shape, which is reached at Na_{39}^- . This is again in agreement with the three models, except for sizes $n=34$ and 35 , where triaxial jellium and CNM incorrectly predict an intermediate change to prolate deformation.

Between Na_{40}^- and Na_{57}^- the picture changes. In the jellium model and the CNM the clusters start oblate and switch to prolate at Na_{45}^- , followed by a transition to a spherical shape at Na_{57}^- . The ellipsoidal model predicts a prolate shape up to $n=52$ and a increasingly triaxially deformed shape up to $n=57$ (in this model the shell closure does not occur at electron number 58 but at 70). In the DFT results the clusters start prolate by continuing the anti-Mackay growth (decorating the anti-Mackay 19 atom double icosahedron²⁴) and switch to oblate at Na_{48}^- when Mackay clusters are energetically favored; finally they transform to a spherical structure at Na_{54}^- . In this comparison one should of course keep in mind that the deformations found for sizes 45–51 might not be the correct ones. Due to the geometric shell closing at size $n=55$ and the electronic shell closing at $n=57$, we observe spherical structures from Na_{54}^- to Na_{57}^- ; a feature missing in the simpler models, which—with the exception of the ellipsoidal model—reach a spherical shape only at Na_{57}^- . Nevertheless the simple models certainly predict the correct tendencies. The very fact that Na_{57}^- adopts a spherical shape by incorporating two atoms into its already closed packed outer layer demonstrates the still rather strong influence of the electronic structure onto the cluster geometry. But one of the most impressive successes of free-electron model predictions can be seen in the structure of Na_{40}^- . This cluster exhibits an

almost isotropic moment of inertia, as can be expected for a size close to an electronic shell closure. Nevertheless it is not spherical, but has a pearlike shape, which is exactly the kind of octupole deformation predicted for this electron number by jellium models.²⁵ The good agreement between PES results and calculated DOS (Fig. 1) demonstrates that this deformation, which up to now has only been seen in a simulation of hot clusters,²⁶ is actually present in the ground state.

Summarizing, the structure of sodium clusters in the range between 20 and 40 atoms is still dominated by electron shell effects, while for larger sizes optimal atomic packing as realized in Mackay icosahedra becomes more important. For certain sizes, however, electronic shell effects still play a significant role.

IV. CONCLUSIONS

The electronic and geometrical structures of sodium cluster anions were determined in the size range from Na_{20}^- to Na_{57}^- by global optimization runs in DFT calculations and the comparison to PES measurements. Together with the recently published results for small clusters with 4–19 atoms⁴ and for larger clusters with up to 309 atoms⁵ these findings lead to a comprehensive understanding of the growth sequence of this prototype of a simple metal cluster system. The intriguing success of simple free-electron models in describing these clusters has been demonstrated but also the limits of these models for clusters beyond Na_{40}^- .

ACKNOWLEDGMENTS

We want to thank A. Eisfeld for calculations of CNM data and Pekka Koskinen for help with the genetic algorithm. This work was supported by the Deutsche Forschungsgemeinschaft. B.H. and M.M. thank the NIC in Jülich and the SCC Karlsruhe for computing grant.

*michael.moseler@iwm.fhg.de

†bernd.von.issendorff@uni-freiburg.de

¹J. A. Alonso, Chem. Rev. (Washington, D.C.) **100**, 637 (2000).

²F. Baletto and R. Ferrando, Rev. Mod. Phys. **77**, 371 (2005).

³K. Koga, T. Ikeshoji, and K.-i. Sugawara, Phys. Rev. Lett. **92**, 115507 (2004).

⁴M. Moseler, B. Huber, H. Häkkinen, U. Landman, G. Wrigge, M. A. Hoffmann, and B. v. Issendorff, Phys. Rev. B **68**, 165413 (2003).

⁵O. Kostko, B. Huber, M. Moseler, and B. von Issendorff, Phys. Rev. Lett. **98**, 043401 (2007).

⁶N. W. Ashcroft and N. D. Mermin, *Solid State Physics* (Saunders College, Philadelphia, PA, 1976).

⁷W. A. de Heer, Rev. Mod. Phys. **65**, 611 (1993).

⁸*Metal Clusters*, edited by W. Ekardt (Wiley&Sons Ltd, Chichester, 1999).

⁹C. Ellert, M. Schmidt, C. Schmitt, T. Reinert, and H. Haberland, Phys. Rev. Lett. **75**, 1731 (1995).

¹⁰R. N. Barnett and U. Landman, Phys. Rev. B **48**, 2081 (1993).

¹¹N. Troullier and J. L. Martins, Phys. Rev. B **43**, 1993 (1991).

¹²J. P. Perdew, K. Burke, and M. Ernzerhof, Phys. Rev. Lett. **77**, 3865 (1996).

¹³I. Rata, A. A. Shvartsburg, M. Horoi, T. Frauenheim, K. W. Michael Siu, and K. A. Jackson, Phys. Rev. Lett. **85**, 546 (2000).

¹⁴The Cambridge Cluster Database, <http://www-wales.ch.cam.ac.uk/CCD.html>

¹⁵G. Wrigge, M. Astruc Hoffmann, and B. v. Issendorff, Phys. Rev. A **65**, 063201 (2002).

¹⁶O. Kostko, N. Morgner, M. A. Hoffmann, and B. v. Issendorff, Eur. Phys. J. D **34**, 133 (2005).

¹⁷H. Haberland, T. Hippler, J. Donges, O. Kostko, M. Schmidt, and B. von Issendorff, Phys. Rev. Lett. **94**, 035701 (2005).

¹⁸C. Yannouleas and U. Landman, Phys. Rev. B **51**, 1902 (1995).

¹⁹K. Selby, M. Vollmer, J. Masui, V. Kresin, W. A. de Heer, and

- W. D. Knight, Phys. Rev. B **40**, 5417 (1989).
- ²⁰K. Clemenger, Phys. Rev. B **32**, 1359 (1985).
- ²¹See EPAPS Document No. E-PRBMDO-80-035947 for the coordinate files. For more information on EPAPS, see <http://www.aip.org/pubserve/epaps.html>
- ²²M. Mundt, S. Kümmel, B. Huber, and M. Moseler, Phys. Rev. B **73**, 205407 (2006).
- ²³H.-P. Cheng, R. S. Berry, and R. L. Whetten, Phys. Rev. B **43**, 10647 (1991).
- ²⁴While a Mackay overlayer continues the fcc stacking of each of the 20 tetrahedra forming an icosahedron, an anti-Mackay overlayer introduces a hexagonal stacking fault.
- ²⁵B. Montag, Th. Hirschmann, J. Meyer, P.-G. Reinhard, and M. Brack, Phys. Rev. B **52**, 4775 (1995).
- ²⁶A. Rytönen, H. Häkkinen, and M. Manninen, Phys. Rev. Lett. **80**, 3940 (1998).